Large-volume flux closure during plasmoid-mediated reconnection in coaxial helicity injection

IOP Publishing | International Atomic Energy Agency Nuclear Fusion

Nucl. Fusion **56** (2016) 044002 (6pp) doi:10.1088/0029-5515/56/4/044002

Letter

Large-volume flux closure during plasmoid-mediated reconnection in coaxial helicity injection

F. Ebrahimi[1] **and R. Raman**[2]

[1] Department of Astrophysical Sciences, and Princeton Plasma Physics Laboratory, Princeton University, NJ 08544, USA
[2] University of Washington, Seattle, WA 98195, USA

E-mail: ebrahimi@princeton.edu

Received 23 December 2015, revised 23 February 2016
Accepted for publication 25 February 2016
Published 23 March 2016

Abstract

A large-volume flux closure during transient coaxial helicity injection (CHI) in NSTX-U is demonstrated through resistive magnetohydrodynamics (MHD) simulations. Several major improvements, including the improved positioning of the divertor poloidal field coils, are projected to improve the CHI start-up phase in NSTX-U. Simulations in the NSTX-U configuration with constant in time coil currents show that with strong flux shaping the injected open field lines (injector flux) rapidly reconnect and form large volume of closed flux surfaces. This is achieved by driving parallel current in the injector flux coil and oppositely directed currents in the flux shaping coils to form a narrow injector flux footprint and push the injector flux into the vessel. As the helicity and plasma are injected into the device, the oppositely directed field lines in the injector region are forced to reconnect through a local Sweet–Parker type reconnection, or to spontaneously reconnect when the elongated current sheet becomes MHD unstable to form plasmoids. In these simulations for the first time, it is found that the closed flux is over 70% of the initial injector flux used to initiate the discharge. These results could work well for the application of transient CHI in devices that employ super conducting coils to generate and sustain the plasma equilibrium.

Keywords: 52.55.Wq, 52.55.Fa, 52.35.Vd, 52.30.Cv

(Some figures may appear in colour only in the online journal)

Helicity-injection current-drive techniques have been utilized to form various types of fusion plasmas through nonaxisymmetric instabilities. In these configurations, as magnetic helicity is injected into the plasma, the additional linkage of the magnetic fluxes can form and sustain the configuration against the resistive decay. Spheromaks [1, 2] and low-aspect-ratio tokamaks [3] are formed through electrostatic helicity injection or so called coaxial helicity injection (CHI). In RFPs, magnetic helicity could be injected steadily by oscillating toroidal and poloidal surface voltages [4, 5]. In all these devices, the core current penetration relies on a relaxation process via current-driven reconnection via nonaxisymmetric instabilities. In a low-aspect-ratio spherical torus (ST) and ST-based fusion reactor, due to the restricted space for a central solenoid, elimination of the central solenoid, and thus non-inductive current-drive techniques, is necessary. Transient CHI is a leading candidate for plasma start-up and current formation in NSTX-U. In NSTX, transient CHI has generated toroidal current on closed flux surfaces without the use of the conventional central solenoid [6]. Unlike the most traditional helicity injection techniques relying on dynamo current drive [7], in transient CHI, the observed good quality

startup current is explained in this letter through simpler axisymmetric reconnection alone. This is advantageous for easier extrapolation of the concept to larger devices. Understanding the physics of magnetic reconnection during CHI, a leading candidate for non-inductive plasma start-up, is of great importance for the viability of this concept for simplifying ST and tokamak based devices by eliminating the central solenoid, as it would provide more flexibility in optimizing the device aspect ratio and improve overall device performance.

Magnetic reconnection, which energizes many processes in nature, is a major interplay for fundamental physical phenomena such as particle acceleration and heating, magnetic-field generation, and momentum transport. Magnetic reconnection also has a critical role in many nonlinear processes of magnetic self-organization, disruption and sawtooth crashes in fusion plasmas. Recently, it has been shown that reconnection could also have a fundamental role in the plasma start up and current formation in NSTX/NSTX-U [8–10]. Using MHD simulations, the fundamental reconnection mechanism that leads to the generation of closed flux surfaces in a transient CHI discharge in NSTX was explained. It was shown that in the right parameter regimes, a local 2D Sweet–Parker type reconnection is triggered in the injector region and closed flux surfaces are formed in the global domain [8, 9]. It was also recognized that transient CHI discharges in NSTX/NSTX-U may provide a rich platform for investigating fundamental reconnection physics in the absence of pre-existing instabilities (kink or tearing), in particular reconnecting-plasmoids physics [10]. Plasmoids can form under different circumstances in fusion and astrophysical plasmas. In the presence of magnetic diffusivity, anytime oppositely directed magnetic field lines in a plasma are forced to reconnect, or pushed together to reconnect via some nonlinear dynamical process, and a long current sheet is formed, the plasmoid instability might occur [11–13] and cause plasmoids to form. For the first time, plasmoid instability in a realistic tokamak geometry was simulated and shown to form during helicity injection in a large fusion device when no other dynamical process (or instability) is initially present. Through resistive magnetohydrodynamics (MHD) simulations, it was demonstrated that during transient CHI discharges at high Lundquist number, the elongated current sheet formed through a Sweet–Parker forced reconnection process breaks up, and a transition to spontaneous reconnection (plasmoid instability) occurs [10]. For a good start-up plasma current, a large fraction of the injected open field lines (injector flux) should rapidly reconnect and form closed flux surfaces. Here, through numerical simulations, we explore the physics of obtaining large volume of flux closure in NSTX-U.

In this letter, we numerically examine the process of fast reconnection and the conversion of large fraction of injected open flux to closed flux surfaces using MHD simulations in the NSTX-U configuration. As in NSTX, transient CHI will be the primary candidate for solenoid-free current start-up in NSTX-U. As shown in figure 1, in CHI, initial poloidal field, the injector-flux (Ψ_{inj}), connecting the inner and outer divertor plates in the injector region is produced using the lower divertor coils (shown with numbers 1, 2 and 3). After gas injection in the divertor region, a voltage (V_{inj}) is applied to the divertor

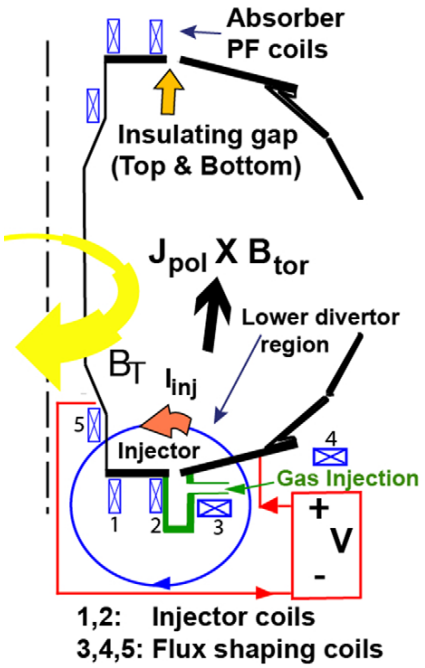

Figure 1. Line drawing showing the main components in NSTX-U required for plasma start-up using CHI. The initial poloidal field, the injector-flux (shown by the blue ellipse), connecting the inner and outer divertor plates in the injector region is produced using the lower divertor coils (shown with numbers 1, 2). The primary injector coil (PF1CL) and the flux shaping coils (PF2L and PF1AL) used in the simulations are shown with numbers 2, 3 and 5, respectively.

plates to drive current along the open field lines, and inject helicity through the linkage of resulting toroidal flux with the poloidal injector flux. NSTX-U will have numerous important upgrades for transient CHI start-up that is projected to significantly increase the CHI current start-up magnitude. The most important of these upgrades is the improved positioning of the divertor coils which allows much better shaping of the injector flux and increases the magnitude of the injector flux by over 2.5 times that in NSTX. Specifically, the injector coil is positioned much closer to the gap between the divertor plates (figure 1).

Here, our simulations, in support of planned experiments, are performed in the NSTX-U geometry by driving current in the lower divertor coils shown in figure 1. Resistive MHD axisymmetric NIMROD simulations for a zero-pressure model are performed with constant in time poloidal-field coil currents to generate the injector and shaping fluxes (fixed-boundary-flux simulations). Similar to NSTX simulations [9], a poloidal grid with 45×90 fifth order finite elements is used in the geometry of NSTX-U. Using the Spitzer resistivity relation with temperature (η (m^2 s^{-1}) $= 410$ T$^{-3/2}$ (eV)), magnetic diffusivity used in the simulations is equivalent to a constant temperature of $T_e \approx 14$ eV, similar to experimental observations in the NSTX.

Helicity injection in the simulations starts by applying a constant voltage $V_{inj} = 800$ V to the inner and outer divertor plates at 6 ms. In the absence of flux shaping coils, the initial

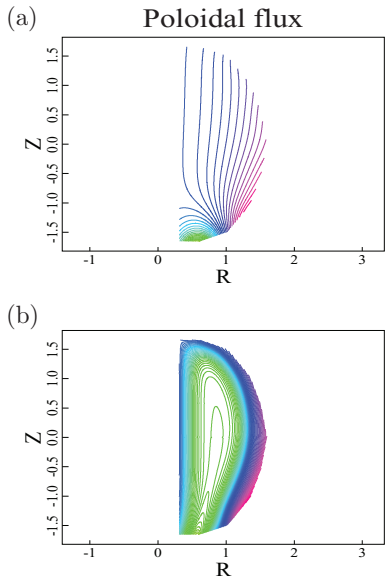

Figure 2. Poloidal flux evolution for NSTX-U simulations without the flux shaping coils. (*a*) Initial poloidal flux ($\Psi_{inj} \sim 70$ mWb) (*b*) at $t = 9$ ms.

poloidal flux shown in figure 2(*a*) is generated with the primary injector coil (PF1CL). Plasma and poloidal flux expand into the device as shown in figure 2(*b*). As the injector voltage is turned off at $t = 9$ ms (decay phase), oppositely-directed field lines in the injector region are pushed together to reconnect and closed flux surfaces are formed. Figure 3(*a*) shows that, as in previous simulations [9], a small volume of closed poloidal flux is formed during the decay phase and open field lines carry most of the current. No current is driven in the flux shaping coils. For this case, the total generated toroidal current is over 300 kA; however, only a small fraction of it, about 10–30% of the current is on closed field lines as shown in figure 3(*b*).

In the next set of simulations, we drive currents in the injector flux shaping coils to bring the injector flux footprints closer together, as it should increase the closed flux fraction [9]. To obtain a narrow injector flux footprint, the currents in the flux shaping coils should be in the opposite direction of current in the primary injector flux coil. The current in the injector coil is in the same direction as the plasma direction. As the injector flux footprint is made narrower, as described in [14], the force balance now requires a larger injector current, because the field line tension increases. This is seen in the simulations,where an injector current of 16 kA is needed for the wide footprint case (figure 3(*b*)), whereas a higher injector current of 34 kA is needed for the narrow flux footprint case. The magnitude of the injector flux for the two cases of wide and narrow flux footprint are 70 mWb and 75 mWb, respectively.

For simulations with narrow flux footprint, after the flux expands and fills up the vessel, a forced Sweet–Parker type reconnection is induced by reducing the injector voltage and current to zero. A much larger volume of flux closure is now formed as shown in figure 4(*a*). Poloidal flux within the last

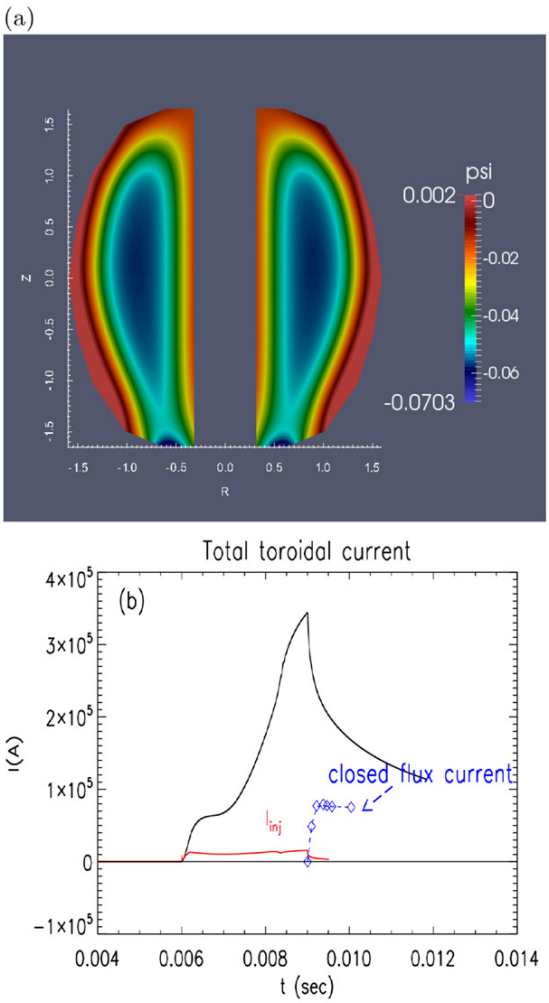

Figure 3. (*a*) Poloidal flux closure during simulations without flux shaping coils ($t = 9.8$ ms). (*b*) Toroidal plasma current, injector current (in red), and closed flux currents (in blue) versus time.

closed flux surface is 40 mWb and, depending on the initial poloidal coil currents, is about 60–70% of the injector flux. In this simulation, due to narrow injection flux footprint and the availability of more reconnecting flux in a narrow region, most of the oppositely-directed open field lines close. In the decay phase, when the injector voltage is off, as the total current starts to resistively decay, almost all of the total current is in the closed flux region (with a large closed-flux current of about 240 kA), as seen in figure 4(*b*). We therefore find that the volume of closed flux surfaces and the closed-flux current with strong flux shaping coils are much larger than the case without flux-shaping coils. The maximum of closed-flux current without the shaping coils is only 20–30% of the total toroidal current and is about a third of the case with flux shaping coils. We should note that the maximum 240 kA closed flux current with strong flux shaping coils is obtained using 140 kA · turns current in the primary injector flux coil. Increasing the current in this coil to the full 318 kA · turns limit should generate more than 400 kA of closed flux current

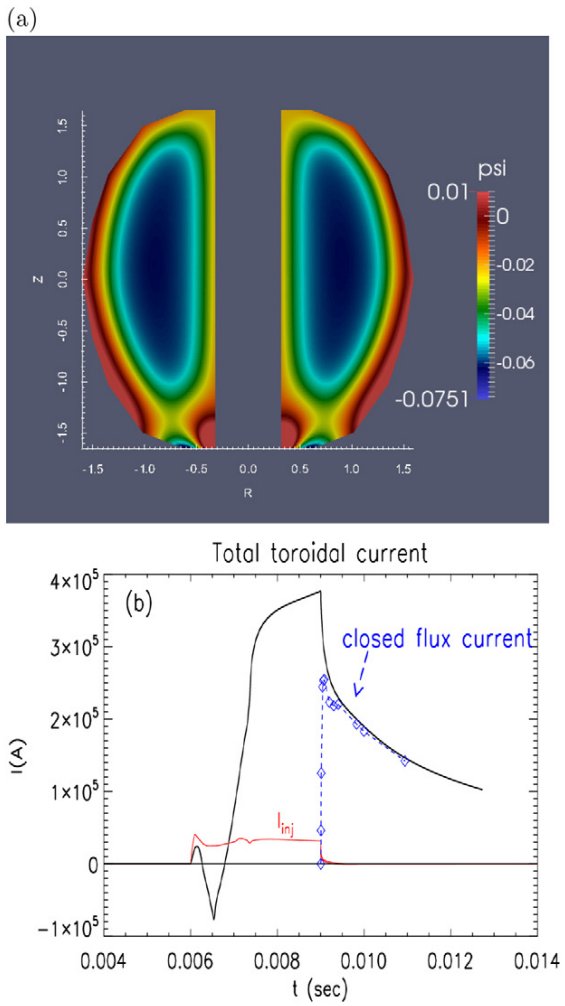

Figure 4. (*a*) Large volume poloidal flux closure during simulations with strong flux shaping coils of PF1AL $= -180$ kA · Turns and PF2L $= -5$ kA · Turns. The current in the primary injector coil (PF1CL) is 140 kA · Turns. at $t = 9.8$ ms. (*b*) Toroidal plasma current, injector current (in red), and closed flux currents (in blue) versus time.

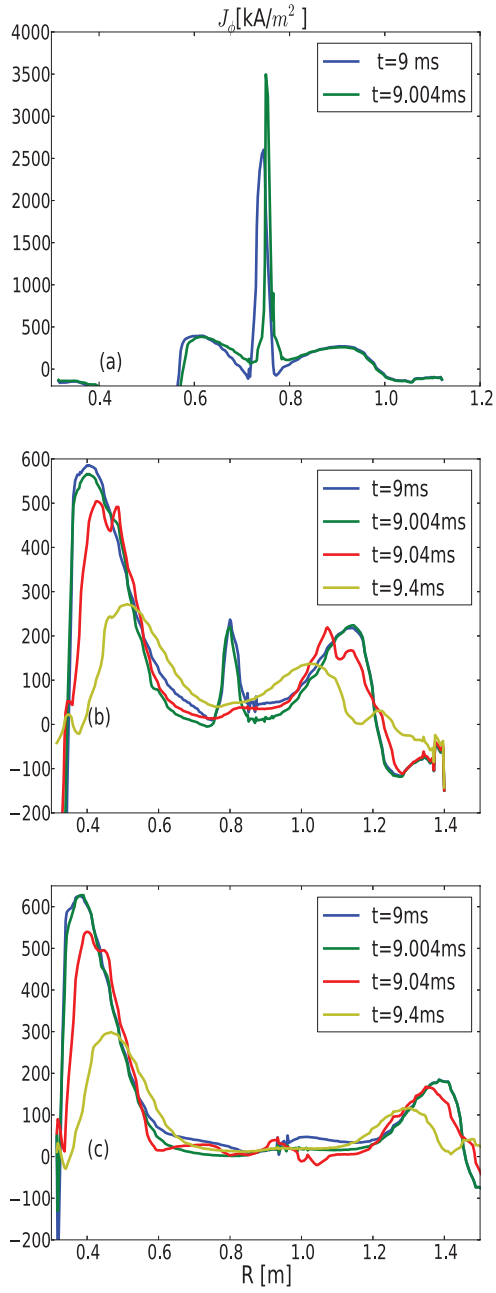

Figure 5. The evolution of current density profiles in time at different vertical locations for the case shown in figure 4(*a*) around the injection region and *x* point formation at $Z = -1.4$ m (*b*) at $Z = -0.9$ m (*c*) at midplane $Z = 0$.

in NSTX-U, as the generated current has been previously shown to be proportional to the injector flux [9].

During the decay phase as the closed flux surfaces are formed, the evolution of current density profiles is shown in figure 5. Around the injection region, as the injection voltage is turned off, the oppositely directed field lines are forced to reconnect and form an elongated current sheet [8]. Formation of a narrow sheet (with a width of about 0.013 m) at $t = 9.004$ ms around $R = 0.75$ m is seen in figure 5(*a*). It should be noted that the current density is relatively localized even during the injection phase with flux shaping coils, however, for this case magnetic reconnection and *x* point formation only occur after $t = 9$ ms. The current densities at other vertical locations are also shown in figures 5(*b*) and (*c*). As the total toroidal current is decaying (after voltage is off), there is also some diffusion of edge current in the core, however as seen in figures 5(*b*) and (*c*) the current density profiles remain mostly hollow (in particular at the mid-plane) during the closed flux formation. The closed-flux current region at $t = 9.4$ ms in figures 5(*b*) and (*c*) is extended in regions around $R = 0.41$–1.36 m and $Z = -1.36$–1.46 m.

To further understand the physics leading to increased flux closure for the case with strong flux shaping, we examine the evolution of poloidal flux during the CHI. The poloidal flux at $t = 7.93$ ms, during the CHI driven phase for a case with flux shaping even stronger than the one for figure 4 is shown in figure 6(*a*). The driven phase is defined as the period when

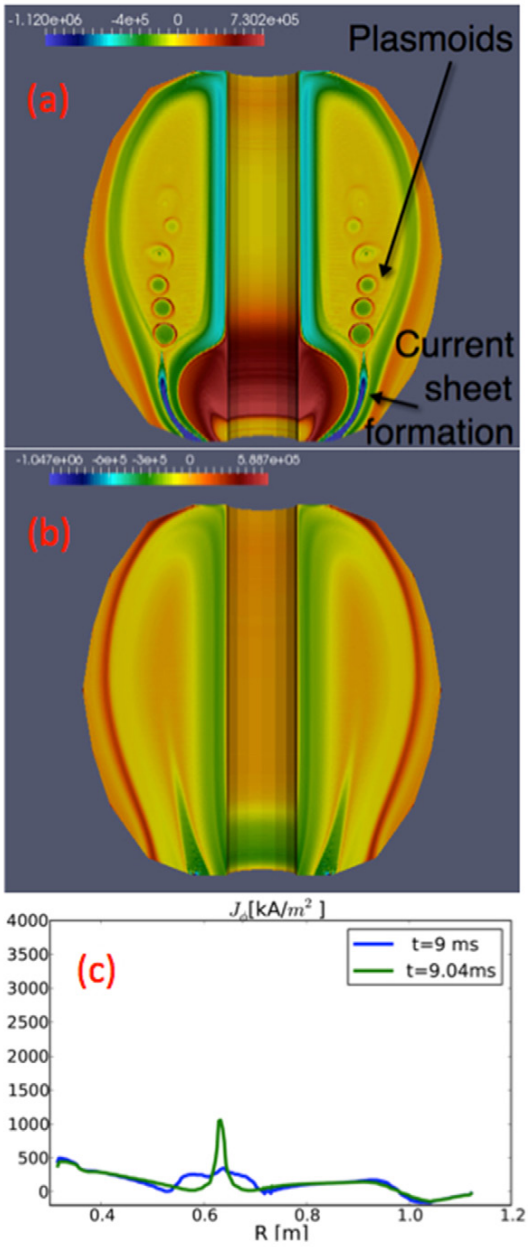

Figure 6. Poloidal R–Z cut of toroidal current densities (J_ϕ) (a) current sheet is formed during the injection phase and magnetic reconnection occurs due to plasmoid instability ($t = 8.04$ ms) in the simulations with further increased PF1AL flux shaping coil currents of 205 kA · Turns. (b) No current sheet formation during the injection phase for the case without flux shaping coils ($t = 8.46$ ms). (c) Current density profiles and current sheet formation at at $Z = -1.4$ m, at 9.0 ms and 9.04 ms (decay phase) for the case without flux shaping coils. Note that the peak current density is less than a third of that in figure 5(a), for the narrow injector flux footprint case.

external voltage is applied to the divertor plates to actively drive current on open field lines. The presence of a thin elongated current sheet and the generation of plasmoids are clearly seen. The elongated current sheet forms due to the combination of a strong reconnecting magnetic field of about 0.05 T, and the narrow injector flux footprint. During this driven phase, the estimated Lundquist number is about 29 000. As described in [10], this is well above the condition for the onset of plasmoid instability in the current sheet. These plasmoids that are formed during the actively driven phase, as described in [10] merge to form large volume closed flux surfaces. For the simulation shown in figure 6(a), the flux shaping is sufficiently strong that the current sheet is plasmoid unstable during the entire injection phase.

The plasmoid instability, however, does not always persist during the entire driven phase. As the flux shaping current is reduced (the case shown in figure 4), the plasmoid instability becomes stable. This is because with a wider flux footprint, the injector flux field line tension decreases, allowing more flux to be injected [1]. This has the tendency to once again widen the current sheet, causing it to become stable to the plasmoid instability. We therefore find that for the case with narrow flux footprint due to very strong shaping, an elongated current forms during the injection phase and magnetic reconnection occurs due to plasmoid instability. However, these plasmoids are transient and their persistence during the injection (driven) phase does depend on the magnitude of the flux shaping current. We note that for the cases with flux shaping, the closed flux current fraction is high even if the plasmoid instability does not persist throughout the driven phase. On the contrary, with wide flux footprint without the flux shaping coils, current sheet is not formed and flux surfaces remain open during the entire injection phase (figure 6(b)). As expected, with wide flux footprint, the current density is radially wide around the injection region during the injection phase ($t = 9$ ms) as shown in figure 6(c). During the decay phase, however, magnetic reconnection occurs and a current sheet is formed as seen in figure 6(c) at $t = 9.04$ ms, and a small volume of flux closure is obtained (figure 3). The current density evolution at other vertical locations during the decay phase, is similar to the case shown in figures 5(b) and (c).

Experimentally, in transient CHI, the injector current is reduced to zero to reduce the open field line currents to zero. This then allows one to unambiguously establish the closed flux current magnitude in experimental discharges. However, it had always been postulated that closed flux surfaces must form and be present at significant levels even before the injector voltage and currents are reduced. Indeed, these simulations show that reconnection occurs during the early injection phase before 9 ms (while the injector voltage is still applied).

In summary, we have performed MHD simulations of transient CHI in the NSTX-U configuration. To explore the effect of the injector flux footprint and achieving the maximum of flux closure, simulations with and without flux shaping coils were performed and compared. Simulations of NSTX-U exhibit similar basic characteristics of flux closure as in NSTX, i.e. a forced Sweet–Parker type reconnection with an elongated current sheet is triggered in the injection region and causes the formation of closed flux surfaces in the global domain. In addition, because of the improved location of injector flux and flux shaping coils in NSTX-U, which allow a better shaping of the initial flux and narrower injector-flux footprints, major improvements and differences are elucidated in the NSTX-U simulations: (1) the volume of flux closure is large and nearly

all of the CHI-generated current is closed-flux current, (2) because of larger reconnecting magnetic field in the injection region, spontaneous reconnection, i.e. plasmoid instability, could occur during the injection phase even at moderate temperatures. First, in the simulations of narrow injector flux footprint generated via better shaping of the initial flux, since there is more available flux (oppositely-directed reconnecting fields) in a narrow region, a larger fraction of open field lines are reconnected and larger volume of flux closure is formed. Second with the narrow flux footprint, local Lundquist number is higher (due to higher accumulation of reconnecting B_z field in the injection region and formation of a longer current sheet), and the transition to plasmoid instability can more easily occur. Simulations show that reconnection could occur at every stage of the helicity injection, but the final resulting state is a large volume of closed flux surfaces at equilibrium with a large CHI-generated closed-flux current. Since constant in time coil currents are used in these simulations, the results suggest that transient CHI should be well suited for use in devices that use superconducting coils in which rapid changes to the coil currents may not be possible.

Acknowledgments

This work was supported by DE-SC0010565, DE-AC02-09CH11466 and DE-FG02-99ER54519. The digital data for this paper can be found in http://arks.princeton.edu/ark:/88435/dsp011v53k0334.

References

[1] Jarboe T.R., Henins I., Sherwood A.R., Barnes C.W. and Hoida H.W. 1983 *Phys. Rev. Lett.* **51** 39
[2] Barnes C.W., Jarboe T.R., Marklin G.J., Knox S.O. and Henins I. 1990 *Phys. Fluids* B **2** 1871
[3] Raman R., Jarboe T.R., Nelson B.A., Izzo V.A., O'Neill R.G., Redd A.J. and Smith R.J. 2003 *Phys. Rev. Lett.* **90** 075005
[4] Ebrahimi F., Prager S.C., Sarff J.S. and Wright J.C. 2003 *Phys. Plasmas* **10** 999
[5] McCollam K.J. *et al* 2010 *Phys. Plasmas* **17** 082506
[6] Raman R. *et al* 2006 *Phys. Rev. Lett.* **97** 175002
[7] Nagata M., Kanki T., Fukumoto N. and Uyama T. 2003 *Phys. Plasmas* **10** 2932
[8] Ebrahimi F., Hooper E.B., Sovinec C.R. and Raman R. 2013 *Phys. Plasmas* **20** 090702
[9] Ebrahimi F., Raman R., Hooper E.B., Sovinec C.R. and Bhattacharjee A. 2014 *Phys. Plasmas* **21** 056109
[10] Ebrahimi F. and Raman R. 2015 *Phys. Rev. Lett.* **114** 205003
[11] Biskamp D. 1986 *Phys. Fluids* **29** 1520
[12] Shibata K. and Tanuma S. 2001 *Earth Planets Space* **53** 473
[13] Loureiro N.F., Schekochihin A.A. and Cowley S.C. 2007 *Phys. Plasmas* **14** 100703
[14] Jarboe T.R. 1989 *Fusion Technol.* **15** 7